

HOSTED BY



Contents lists available at ScienceDirect

Journal of King Saud University – Science

journal homepage: www.sciencedirect.com



Original article

Zinc oxide Nanoparticles, Biosynthesis, characterization and their potent photocatalytic degradation, and antioxidant activities



Fawziah M. Albarakaty^a, Mayasar I. Alzaban^b, Nada K. Alharbi^b, Fatima S. Bagrwan^b,
Abeer R.M. Abd El-Aziz^c, Mohamed A. Mahmoud^{c,*}

^a Department of Biology, Faculty of Applied Science, Umm Al-Qura University, P.O. Box 715, Makkah Al Mukarramah, Saudi Arabia

^b Department of Biology, College of Science, Princess Nourah bint Abdulrahman University, P.O. Box 84428, Riyadh 11671, Saudi Arabia

^c Molecular Markers Laboratory, Plant Pathology Research Institute, Agricultural Research Center, Giza 12619, Egypt

ARTICLE INFO

Article history:

Received 28 September 2022

Revised 26 October 2022

Accepted 3 November 2022

Available online 9 November 2022

Keywords:

ZnO nanoparticles

Moringa oleifera

Physicochemical properties

Photocatalytic and antioxidant activity

ABSTRACT

Objectives: This study aimed to biosynthesize zinc oxide nanoparticles (ZnO-NPs) using the seed extract of *Moringa oleifera*. The catalytic activity of the biosynthesized ZnO-NPs was examined as photocatalyst for the degradation methylene blue (MB) and their antioxidant activity by H₂O₂ assay were studied.

Methods: The biosynthesized ZnO-NPs and their physicochemical properties investigated via UV-visible spectroscopy (UV-vis), Fourier transform infrared (FTIR) spectroscopy, Transmission electron microscopy (TEM), energy dispersive X-ray (EDX), X-ray diffraction analysis (XRD) analysis, and zeta potential was calculated using the Zetasizer nano.

Results: UV-Visible analysis of the biosynthesized nanoparticles revealed the characteristic a specific peak at 375 nm indicating the formation of ZnO-NPs. XRD study showed a distinctive diffraction peak indicating the formation of crystalline nanoparticles which matches to the spherical and hexagonal structure of ZnO-NPs. TEM results confirmed the formation of spherical and hexagonal ZnO-NPs and the size ranging between 25 and 30 nm. EDX analysis was used for the determination of elemental composition of biosynthesized ZnO-NPs which included zinc, oxygen and carbon. FTIR spectroscopy is useful to determine the available functional group from the phytochemical components implicated in the stabilization and reduction of ZnO-NPs. ZnO-NPs exhibited effective photocatalytic activity in degrading methylene blue (MB) and maximum photocatalytic activity (71 %) after 24 hrs. In addition, ZnO NPs exhibited high antioxidant activity against H₂O₂ free radicals scavenger.

Conclusion: The biosynthesized ZnO-NPs have excellent MB dye degradation power and complete dye degradation was achieved within 24 hrs and synthesized ZnO-NPs showed improved antioxidant power. ZnO-NPs are good tools for industrial applications.

© 2022 The Author(s). Published by Elsevier B.V. on behalf of King Saud University. This is an open access article under the CC BY-NC-ND license (<http://creativecommons.org/licenses/by-nc-nd/4.0/>).

1. Introduction

Zinc oxide (ZnO) is one of the important chemical compounds received much more attention in recent years due to its potential properties in various applications, such as photonics, cosmetics, pharmaceuticals and photocatalysis (Yusof et al., 2020; Podasca

and Damaceanu 2020; Oh and Kim 2019; Lee et al., 2019), optical, piezoelectric, magnetic, and gas-sensing (Seshadri et al., 2004), bioremediation of wastewater, and as a potential antimicrobial property (Wang et al., 2004; Azizi et al., 2016). ZnO nanoparticles (ZnO-NPs) are synthesized using various methods, including sol-gel processes, ball milling, microemulsion and laser vaporization method (Hernández et al., 2020; Abdolhoseinzadeh and Sheibani, 2020). Generally, these nanoparticles preparation methods face several limitations, including, high cost state of art experiments, man power, and required very large area for the installation of equipments, and toxic chemicals, addition capping agent and stabilizers (Yusof et al., 2019). Almost all chemical methods are harmful to the environment because of the use of various chemicals for nanoparticles stabilization process and the chemicals bind with nanoparticles and affect various biological properties (Ielo et al.,

* Corresponding author.

E-mail addresses: fimbarakati@uqu.edu.sa (F.M. Albarakaty), m.a.mahmoud75@gmail.com (M.A. Mahmoud).

Peer review under responsibility of King Saud University.



Production and hosting by Elsevier

<https://doi.org/10.1016/j.jksus.2022.102434>

1018-3647/© 2022 The Author(s). Published by Elsevier B.V. on behalf of King Saud University.

This is an open access article under the CC BY-NC-ND license (<http://creativecommons.org/licenses/by-nc-nd/4.0/>).

2021). Whereas, nanoparticles synthesis by green-synthesis approach is generally considered as safe, bio-compatible and non-toxic to the organism or environment (Lakshmeesha et al., 2014). Additionally, green synthesis method has various advantages, such as simple method, less time consumed, low-cost and high purity.

Several varieties of plant and fruit extracts were employed for the biosynthesis of ZnO-NPs, namely, *Salvadora oleoides*, *Echinacea* spp., and *Boswellia ovalifoliolata*, and *Ocimum Americanum* (Supraja et al., 2016, Padalia et al., 2017, Attar and Yapaöz, 2018, Kumar et al., 2019).

Eco-friendly ZnO-NPs were used as photocatalytic agents for many organic dyes, such as methylene blue (MB) dye, which degraded (88 %) in 140 min (Supraja et al., 2016) also, Padalia et al. (2017) and his team degraded up to 86 % in 180 min. The photocatalytic assessment proved the ZnO-NPs achieved 100 % elimination of MB dye at 60 min exposure, and 85 and 92 % degradation of methyl orange (MO) and Rhodamine B (RhB), respectively, at 180 min (Karaköse et al. 2018).

In this study, *M. oleifera* aqueous seed extract was used for the biosynthesis of ZnO-NPs. The photocatalytic activity against methylene blue dye and antioxidant potential are assayed.

2. Materials and methods

2.1. Preparation of seed extract and green-synthesis of ZnO NPs

The seeds of *Moringa oleifera* were removed from the pods and crushed using a mechanical blender. A total of 10 g of seeds were powdered using a pestle and mortar and stirred with 100 mL double distilled water. It was placed on a heating mantle and stirred manually for 25 min at 80 ± 2 °C. The final aqueous extract was cooled and it was filtered (Whatman filter No: 1). The filtrate was collected and used as a reducing and capping agent for the green synthesis of ZnO NPs. A total of 5 gm of zinc nitrate hexahydrate [$\text{Zn}(\text{NO}_3)_2 \cdot 6\text{H}_2\text{O}$] (Sigma-Aldrich, USA) was mixed with aqueous extract for 2 hrs and the development of brownish-yellow was monitored. The sample was maintained on a heating mantle at 70 ± 2 °C for 6 hrs to produce white ZnO-NPs. The mixture was centrifuged for 15 min at 8000 rpm and the sediment sample was retained. It was calcined for 2 hrs at 400 ± 2 °C and a white crystalline powder was obtained. It was stored in an amber color bottle for further analysis (Azizi et al., 2014).

2.2. Characterization

UV-visible spectrophotometer analysis was performed to analyze the absorption spectra range of the sample at 200–800 nm (Victoria, Australia). X-ray diffraction analysis (XRD) was used to determine the particle distribution, particle size and shape heterogeneity of ZnO-NPs. The white crystalline ZnO-NPs were used for characterization studies. The powder sample tested using X'pert PRO PANalytical diffract meter. FT-IR analysis was performed to analyze the functional group of ZnO-NPs range from 4000 to 400 cm^{-1} . Transmission electron microscopy (TEM) analysis was used to study the morphology of ZnO-NPs (JEOL model JEM-1010, Tokyo, Japan). X-ray spectroscopy (EDX) analysis was performed to determine elements using Shimadzu DX-700HS machine. The zeta potential was calculated using the Zetasizer nano array, HT Laser, ZEN 3600 (Malvern Instruments, UK) with a dispersion angle and a temperature of 90 °C and 25 °C, respectively, using samples diluted with de-ionized distilled water at different concentrations.

2.3. Catalytic activity

In our study, photocatalytic activity of ZnO-NPs was analyzed against an azo dye, methylene blue. Experiment was performed under UV light (366 nm). The initial methylene blue concentration was 50 ppm and 0.02 % ZnO-NPs was incorporated in a 100 mL beaker, under UV irradiation at 35 ± 1 °C. It was stirred continuously to achieve homogeneity of the sample. The absorbance of the sample was measured at 660 nm using a UV-visible spectrophotometer.

2.4. Antioxidant activity

Hydrogen peroxide (H_2O_2) free radical scavenging activity of the nanoparticles was performed as described previously (Pick and Mizel, 1981). The green synthesized ZnO-NPs was tested at various concentrations and the final reaction volume was 1 mL. To the ZnO-NPs, 0.6 mL (50 mM) H_2O_2 stock solution was added and incubated for 5 min at 28 ± 2 °C. Phosphate-buffered saline alone was considered as the blank. After 5 min incubation, hydrogen peroxide scavenging power (%) was determined using the following formula:

$$\% \text{H}_2\text{O}_2 \text{ free radicals} = 1 - \text{As}/\text{Ac} \times 100.$$

where Ac = Control absorbance; As = test absorbance.

3. Result and discussion

3.1. UV-visible spectrophotometer analysis

In Fig. 1a, pure ZnO-NPs as a white powder is shown, which reveals the development of nanoparticles in an early stage. The green synthesized nanoparticles were white crystalline nature and used for the determination of absorption spectra. In our study, a major peak was detected at 375 nm, which indicated the presence of ZnO-NPs (Fig. 1b).

3.2. XRD analysis

The green synthesized ZnO-NPs were subjected for XRD analysis to determine crystalline structure. The XRD pattern of ZnO-NPs was described in Fig. 2. The number of Bragg reflections for ZnO-NPs using aqueous extract of *M. oleifera* matter appears at $2\theta = 3.180^\circ, 34.45^\circ, 36.28^\circ, 47.59^\circ, 56.65^\circ, 62.94^\circ, 66.46^\circ, 68.00^\circ, 69.09^\circ, 72.57^\circ$ and 77.0648° which correspond to the reflection from (100), (002), (101), (102), (110), (103), (200), (112), (201), to (004) respectively. The present finding showed good agreement with previous results revealed hexagonal wurtzite structure of ZnO-NPs (Swee-Yong et al., 2012).

3.3. TEM image

The shape and size of the green synthesized ZnO-NPs were analyzed using TEM analysis and the result was described in Fig. 3. Fig. 3 clearly shows the spherical structure of NPs and the size ranging between 25 and 30 nm. Most of the analyzed particles were almost uniform in size. The mean value of the green synthesized ZnO-NPs was 28 nm. The present finding revealed the potential of seed extract as reducing and capping agent. The spherical and hexagonal structures of NPs were in accordance with previous results reported by Liu et al., (2017) and Malviya (2011).

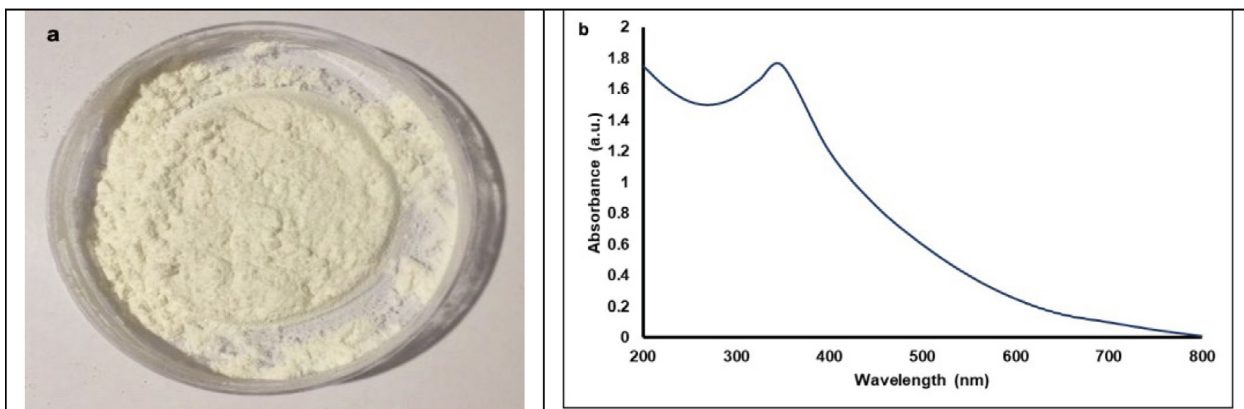


Fig. 1. A) pure ZnO-NPs as a white powder, b) UV–visible spectrum of ZnO-NPs synthesized using seed extract of *M. oleifera*.

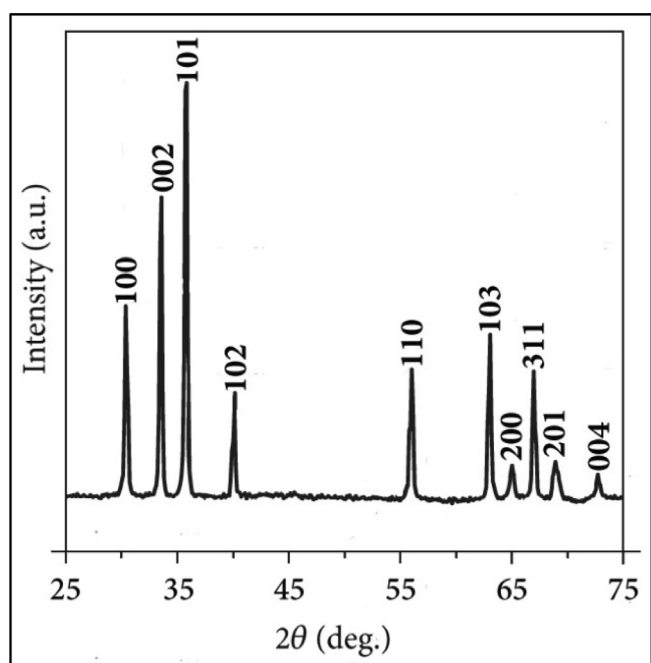


Fig. 2. XRD pattern of ZnO-NPs synthesized using aqueous seed extract of *M. oleifera*.

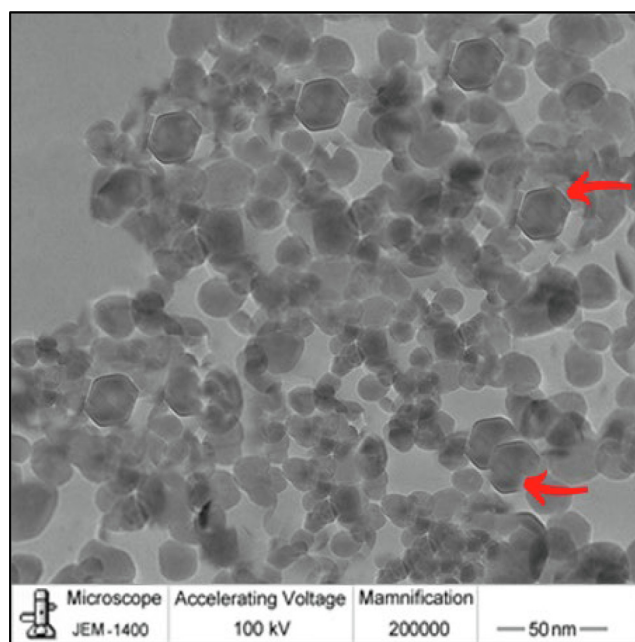


Fig. 3. TEM of ZnO-NPs.

3.4. EDX analysis

EDX analysis was used for the determination of elemental composition of biosynthesized ZnO-NPs and the result was depicted in Fig. 4. In our study, the presence of oxygen and zinc components was determined in EDX spectrum. The ZnO-NPs element characterization revealed 86.79 % zinc, 10.48 % oxygen and 2.73 carbon 2.73 for weight %67.27 % zinc, 25.81 % oxygen and 6.92 % carbon.

3.5. Zeta-potential

Zeta-potential analysis was performed to determine the stability and surface charge of the particles of interest. The zeta potential of ZnO-NPs revealed the presence of a major peak at -38 mV revealed good stability of the particle (Fig. 5). The present finding clearly revealed that the capping agent from the plant source is circled with ZnO-NPs. Naturally, the selected plant seed contains rich

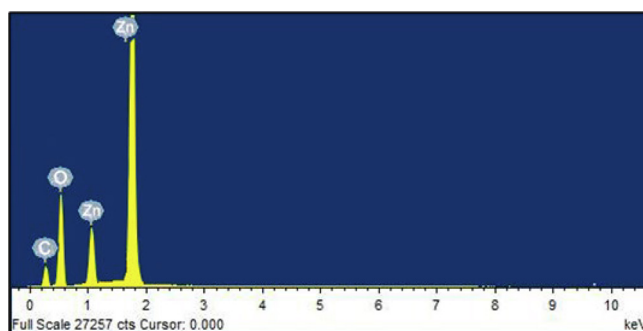


Fig. 4. EDX analysis of ZnO-NPs.

of flavonoids and proteins and these phytochemical components involved in the reduction of metal ions and good stabilization of ZnO-NPs. Our findings were highly consistent with (Kaur et al., 2022).

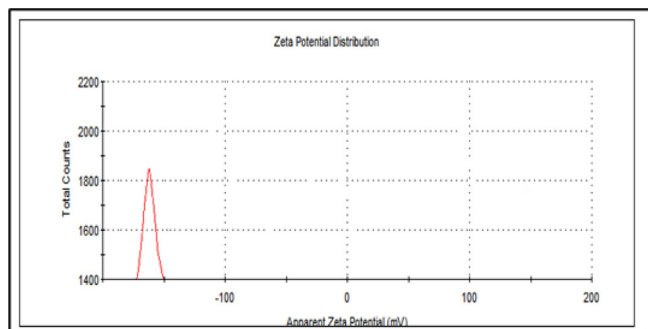


Fig. 5. Zeta potential of ZnO-NPs.

3.6. FTIR analysis

FTIR analysis was carried out for the ZnO-NPs detection of biomolecules responsible for biosynthesized ZnO-NPs. FTIR analysis is useful to determine the available functional group from the phytochemical components implicated in the stabilization and reduction of ZnO-NPs. The comparative FTIR spectrum of *M. oleifera* seed extract and green synthesized NPs revealed the functional group of seed extract (Fig. 6). *M. oleifera* seed extract showed various peaks at 3420, 2923, 2852, 1800, 1740, 1715, 1685, and 1492 cm^{-1} . The absorption band at 3420 cm^{-1} (strong O–H stretching) established fatty acids, protein, and carbohydrate molecules. At this region N–H stretching was observed because of increased protein content from the seed (Stuart et al., 2004). Two peaks detected at 2852 cm^{-1} , 2923 cm^{-1} and this wave number indicated symmetric and asymmetric stretching related to C–H bonding. The intensity of these bonding was high, which revealed the presence of lipid similar with protein content (Krilov et al., 2009).

In our study various overlapping bands were detected from 1750 to 1630 cm^{-1} . This mainly due to the presence of C=O stretching. The carbonyl group (C=O) detected in the FTIR analysis related to the protein part and fatty acid content of the aqueous seed extract. The small absorption bands at 1740 and 1715 cm^{-1} region revealed carbonyl groups and the band at 1658 cm^{-1} revealed carbonyl amides.

The FTIR analysis of the green NPs synthesized using aqueous seed extract revealed specific changes in related peaks, indicating the presence of capping agent or bonded to the NPs surface. In the seed extract the major peaks were detected appeared at

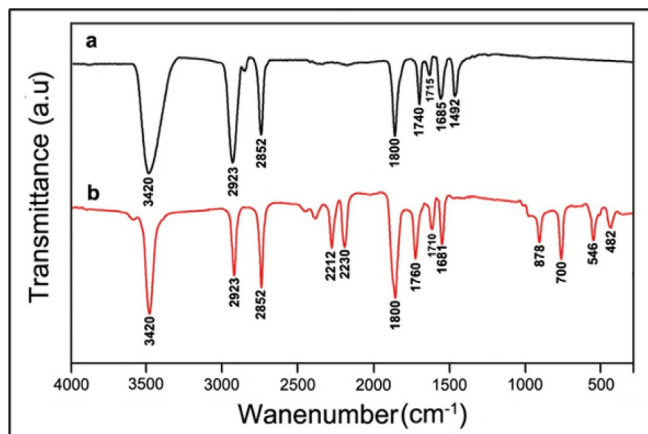


Fig. 6. FTIR spectrum of a) *M. oleifera* seed extract, and b) biosynthesized ZnO-NPs.

3420, 2923, 2852, and 1800 cm^{-1} appear with no change in ZnO-NPs, while other peaks shifted from 1740, 1715, and 1685 cm^{-1} to 1760, 1710, and 1681 cm^{-1} respectively, were ascribed to N–H binding. A shift of peaks was observed between these two FTIR spectrum revealed the interaction of various functional groups of the phenols and flavonoids with the green synthesized ZnO-NPs. The available functional group from the seed extract donated electrons and these electrons reduced zinc ions (Zn^{2+}) to Zn^{+1} and finally reduced as zinc NPs. The seed extract contains negative functional group and working as a stabilizing agent. The appearance of new peaks at 2212, 2230, 878, 700, 546, and 482 cm^{-1} revealed that ZnO-NPs participated C=C, and C–H bending, and the peak at 482 cm^{-1} revealed bending vibration (Selim et al., 2020). An intense and sharp band was observed at 546 cm^{-1} , revealing the presence of Zn–O vibrations and a peak at 878 cm^{-1} showed the existence of the weak vibration (Stan et al., 2016). In general, the metal oxides show very strong absorption bands with the wave number < 1000 cm^{-1} (Kaviyarasu et al., 2016; Ngom et al., 2016; Bhuyan et al., 2016). In ZnO-NPs, intrinsic absorption peak was observed at 481 cm^{-1} , which revealed the presence of stretching mode and OH group also determined at higher wave numbers (Nethravathi et al., 2015).

3.7. Dye degradation under UV radiation

Photocatalytic technology is a critical method for eliminating dyes in sewage water. In our study, azo dye degradation was observed by analyzing the color shift. After 6 h incubation of MB with green synthesized ZnO-NPs, the color of dye changed to light blue from the initial dark blue coloration after UV exposure (Fig. 7a). After 12 h of incubation, the light blue color changed into light green color. After 24 h, degradation was achieved completely and the final solution was colorless. It is very clear that the absorption peak reduced considerably after 24 hrs incubation revealed UV-mediated photocatalytic reaction (Fig. 7b). The green synthesized ZnO-NP effectively reduced the color intensity, revealed the dye degradation efficacy. The dye degradation kinetics as a function of incubation time was depicted in Fig. 7c. The present study revealed maximum photocatalytic activity (71 %) after 24 hrs incubation. Nava et al., (2017) have been biosynthesized ZnO-NPs using *Camellia sinensis* extract and used for the degradation of MB and achieved about 80 % degradation within two hours. Likewise, 80 % degradation was achieved within 120 min using silver nanoparticles (Al-Zaban et al., 2021). In photocatalytic reaction, under UV irradiation condition, electron shift was observed. In general, oxidizing species can oxidize various organic pollutants. The photocatalytic activity of nanoparticles and the final products was mainly based on the number of defects (Ngoepe et al., 2018; Liang et al., 2020).

3.8. Antioxidant properties

The antioxidant properties of green synthesized ZnO-NPs were described Fig. 8. ZnO-NPs showed H_2O_2 reducing power activity and were dose dependent. The IC₅₀ value of ZnO-NPs was 62 $\mu\text{g}/\text{mL}$, whereas the standard ascorbic acid showed decreased IC₅₀ value (43 $\mu\text{g}/\text{mL}$). The antioxidant activity was high in ZnO-NPs than seed extract which revealed the presence of metallic structure. Medicinal plants contain various phenolic compounds and these compounds contributed antioxidant property (Arvanag et al., 2019). The green synthesized ZnO-NPs from the extracts of *Ocimum basilicum*, *Rosmarinus officinalis* and *Allium sativum* showed strong antioxidant activity (Parashant et al., 2015).

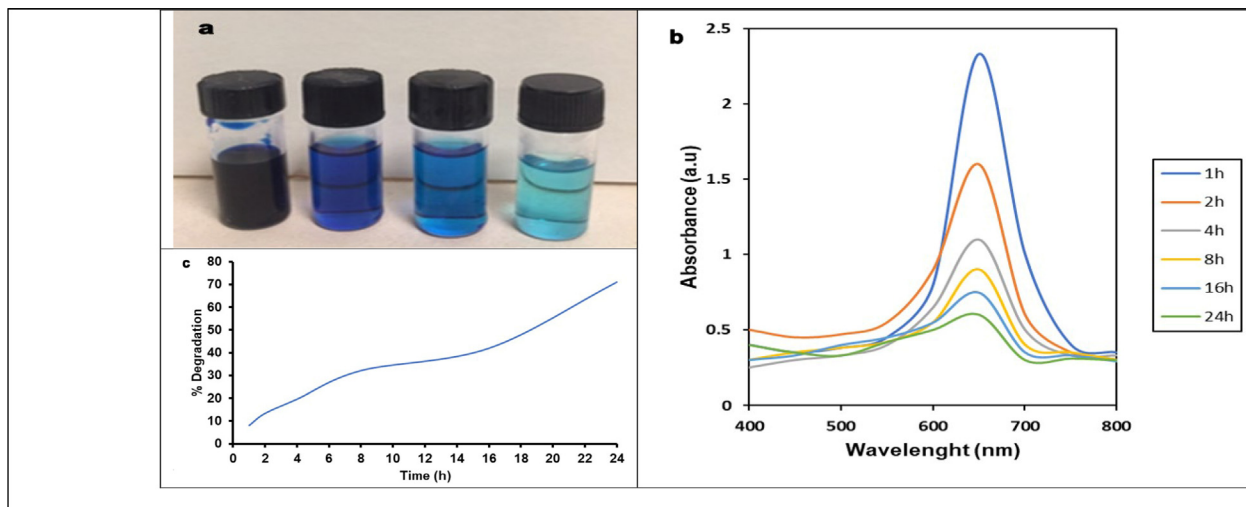


Fig. 7. Catalytic activity of ZnO-NPs synthesized using seed extract of *M. oleifera* under UV radiation.

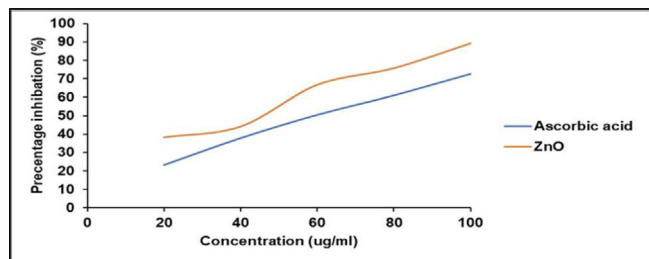


Fig. 8. Antioxidant activity of green synthesized ZnO-NPs at various concentrations. Hydrogen peroxide reducing power was analyzed and compared with standard (ascorbic acid).

4. Conclusions

Green synthesis of ZnO-NPs using plant extract is cost-effective, safe and simple to obtain uniform size ZnO-NPs crystal. The biosynthesized NPs were functionally characterized and the role of plant extract as reducing and capping power was tested using UV-vis spectroscopy analysis, FT-IR spectroscopy, and XRD. The mean nanoparticles size was about 28 nm revealed the positive role of seed extract as a capping agent and the size of the nanoparticles was also almost uniform. The XRD analysis revealed the purity of crystalline ZnO-NPs and the seed extract has the potential to contribute reduction reaction. The biosynthesized ZnO-NPs have excellent MB dye degradation power and complete dye degradation was achieved within 24 hrs. The green synthesized ZnO-NPs showed improved antioxidant power.

Declaration of Competing Interest

The authors declare that they have no known competing financial interests or personal relationships that could have appeared to influence the work reported in this paper.

Acknowledgments

Princess Nourah bint Abdulrahman University Researchers Supporting Project number (PNURSP2022R84), Princess Nourah bint Abdulrahman University, Riyadh, Saudi Arabia.

References

- Abdohoseinzadeh, A., Sheibani, S., 2020. Enhanced photocatalytic performance of Cu_2O nano-photocatalyst powder modified by ball milling and ZnO. *Adv. Powder Technol.* 31, 40–50. <https://doi.org/10.1016/j.apt.2019.09.035>.
- Al-Zaban, M.I., Mahmoud, M.A., Al-Harbi, M.A., 2021. Catalytic degradation of methylene blue using silver nanoparticles synthesized by honey. *Saudi J. Biol. Sci.* 28, 2007–2013. <https://doi.org/10.1016/j.sjbs.2021.01.003>.
- Arvanag, F.M., Bayrami, A., Habibi-Yangjeh, A., Pouran, S.R., Mohammadi, F., Pouran, C., 2019. A comprehensive study on antidiabetic and antibacterial activities of ZnO nanoparticles biosynthesized using *Silybum marianum* L. seed extract. *Mater. Sci. Eng. C* 97, 397–405. <https://doi.org/10.1016/j.msec.2018.12.058>.
- Attar, A., Yapaöz, M.A., 2018. Biomimetic synthesis, characterization and antibacterial efficacy of ZnO and Au nanoparticles using echinacea flower extract precursor. *Mater. Res. Express* 5, 055403.
- Azizi, S., Ahmad, M.B., Namvar, F., Mohamad, R., 2014. Green biosynthesis and characterization of zinc oxide nanoparticles using brown marine macroalgae *Sargassum muticum* aqueous extract. *Mater. Lett.* 116, 275–277. <https://doi.org/10.1016/j.matlet.2013.11.038>.
- Azizi, S., Ahmad, M.B., Hussein, M., Zobir, A., Ibrahim, N.A., 2016. Synthesis, antibacterial and thermal studies of cellulose nanocrystal stabilized ZnO-Ag heterostructure nanoparticles. *Molecules* 18, 626. <https://doi.org/10.3390/molecules18066269>.
- Bhuyan, B., Paul, B., Purkayastha, D.D., Dhar, S.S., Behera, S., 2016. Facile synthesis and characterization of zinc oxide nanoparticles and studies of their catalytic activity towards ultrasound-assisted degradation of metronidazole. *Mater. Lett.* 168, 158–162. <https://doi.org/10.1016/j.matlet.2016.01.024>.
- Hernández, R., Hernández-Reséndiz, J.R., Martínez-Chávez, A., Velázquez-Castillo, R., Escobar-Alarcón, L., Esquivel, K., 2020. X-ray diffraction Rietveld structural analysis of Au-TiO₂ powders synthesized by sol-gel route coupled to microwave and sonochemistry. *J. Sol-Gel Sci. Technol.* 93, 1–14. <https://doi.org/10.1007/s10971-020-05264-5>.
- Ielo, I., Rando, G., Giacobello, F., Sfameni, S., Castellano, A., Galletta, M., Drommi, D., Rosace, G., Plutino, M.R., 2021. Synthesis, chemical-physical characterization, and biomedical applications of functional gold nanoparticles: a review. *Molecules* 26, 5823. <https://doi.org/10.3390/molecules26195823>.
- Karaköse, E., Çolak, H., 2018. Structural, electrical, and antimicrobial characterization of green synthesized ZnO nanorods from aqueous *Mentha* extract. *MRS Commun.* 8, 577–585.
- Kaur, J., Anwer, M.K., Sartaj, A., Panda, B.P., Ali, A., Zafar, A., Kumar, V., Gilani, S.J., Kala, C., Taleuzzaman, M., 2022. ZnO nanoparticles of *Rubia cordifolia* extract formulation developed and optimized with qbd application, considering ex vivo skin permeation, antimicrobial and antioxidant properties. *Molecules* 27, 1450. <https://doi.org/10.3390/molecules27041450>.
- Kaviyarasu, K., Fuku, X., Mola, G.T., Manikandan, E., Kennedy, J., Maaza, M., 2016. Photoluminescence of well-aligned ZnO doped CeO₂ nanoplatelets by asolvothermal route. *Mater. Lett.* 183, 351–354. <https://doi.org/10.1016/j.matlet.2016.07.143>.
- Krilov, D., Balarin, M., Kosović, M., Gamulin, O., Brnjac-Kraljević, J., 2009. FT-IR spectroscopy of lipoproteins—a comparative study. *Spectrochimica Acta Part A* 73, 701–706. <https://doi.org/10.1016/j.saa.2009.03.015>.
- Kumar, H.K.N., Mohana, N.C., Nuthan, B.R., Ramesha, K.P., Rakshith, D.R., Geetha, N., Satish, S., 2019. Phyto-mediated synthesis of zinc oxide nanoparticles using aqueous plant extract of *Ocimum americanum* and evaluation of its bioactivity. *SN Appl. Sci.* 1, 651. <https://doi.org/10.1007/s42452-019-0671-5>.

- Lakshmeesha, T.R., Sateesh, M.K., Daruka, P.B., Sharma, S.C., Kavyashree, D., Chandrasekhar, M., Nagabhushana, H., 2014. Reactivity of crystalline ZnO superstructure against fungi and bacteria pathogens: synthesized using Nerium oleander leaf extract. *Cryst. Growth disease* 14, 4068–4079. <https://doi.org/10.1021/cg500699z>.
- Lee, C.G., Na, K.H., Kim, W.T., Park, D.C., Yang, W.H., Choi, W.Y., 2019. TiO₂/ZnO nanofibers prepared by electrospinning and their photocatalytic degradation of methylene blue compared with TiO₂ nanofibers. *Appl. Sci.* 9, 3404. <https://doi.org/10.3390/app9163404>.
- Liang, H., Tai, X., Du, Z., Yin, Y., 2020. Enhanced photocatalytic activity of ZnO sensitized by carbon quantum dots and application in phenol wastewater. *Opt. Mater.* 100. <https://doi.org/10.1016/j.optmat.2020.109674>
- Liu, S., Long, Q., Xu, Y., Wang, J., Xu, Z., Wang, L., Zhou, M., Wu, Y., Chen, T., Shaw, C., 2017. Assessment of antimicrobial and wound healing effects of Brevinin-2Ta against the bacterium *Klebsiella pneumoniae* in dermally-wounded rats. *Oncotarget* 8, 111369–111385. <https://doi.org/10.18632/oncotarget.22797>.
- Malviya, S., 2011. Medicinal attributes of *Acacia nilotica* Linn. - A comprehensive review on ethnopharmacological claims. *Int. J. of Pharm. and Life Sci.* 2, 830–837.
- Nava, O., Morales, P.L., Gutiérrez, C.M.G., Vilchis-Nestor, A., Castro-Beltrán, A., Mota-González, M., Olivas, A., 2017. Influence of *Camellia sinensis* extract on zinc oxide nanoparticle green synthesis. *J. Mol. Struct.* 1134, 121–125. <https://doi.org/10.1016/j.molstruc.2016.12.069>.
- Nethravathi, P.C., Shruthi, G.S., Suresh, D., Udayabhanu, A., Nagabhushana, H., Sharma, S.C., 2015. *Garcinia xanthochymus* mediated green synthesis of ZnO nanoparticles: photoluminescence, photocatalytic and antioxidant activity studies. *Ceram. Int.* 41, 8680–8687. <https://doi.org/10.1016/j.ceramint.2015.03.084>.
- Ngope, N., Mbita, Z., Mathipa, M., Mketi, N., Ntsendwana, B., Hintsho-Mbita, N., 2018. Biogenic synthesis of ZnO nanoparticles using *Monsonia burkeana* for use in photocatalytic, antibacterial and anticancer applications. *Ceram. Int.* 44, 16999–17000. <https://doi.org/10.1016/j.ceramint.2018.06.142>.
- Ngom, B.D., Mpahane, T., Manikandan, E., Maaza, M., 2016. ZnO nano-discs by lyophilization process: size effects on their intrinsic luminescence. *J. Alloys Compd.* 656, 758–763. <https://doi.org/10.1016/j.jallcom.2015.09.230>.
- Oh, S., Kim, J., 2019. Correlation between the morphology of ZnO layers and the electroluminescence of quantum dot light-emitting diodes. *Appl. Sci.* 9, 4539. <https://doi.org/10.3390/app9214539>.
- Padalia, H., Baluja, S., Chanda, S., 2017. Effect of pH on size and antibacterial activity of *Salvadora oleoides* leaf extract-mediated synthesis of zinc oxide nanoparticles. *BioNanoScience* 7, 40–49. <https://doi.org/10.1007/s12668-016-0387-6>.
- Parashant, G.K., Prashant, P.A., Utpal, B., Manoj, G., Nagabhushana, B.M., Ananda, S., Krishnaiah, G.M., Sathyananda, H.M., 2015. In vitro antibacterial and cytotoxicity studies of ZnO nanoparticles prepared by combustion assisted facile green synthesis. *Karbala Int. J. Mod. Sci.* 1, 67–77. <https://doi.org/10.1016/j.kijoms.2015.10.007>.
- Pick, E., Mizel, D., 1981. Rapid microassays for the measurement of superoxide and hydrogen peroxide production by macrophages in culture using an automatic enzyme immunoassay reader. *J. Immunol. Methods* 46, 211–226. [https://doi.org/10.1016/0022-1759\(81\)90138-1](https://doi.org/10.1016/0022-1759(81)90138-1).
- Podasca, V.E., Damaceanu, M.D., 2020. Photopolymerized films with ZnO and doped ZnO particles used as efficient photocatalysts in malachite green dye decomposition. *Appl. Sci.* 10, 1954. <https://doi.org/10.3390/app10061954>.
- Selim, Y.A., Maha, A.A., Ragab, I., Abd El-Aziz, M.H.M., 2020. Green synthesis of zinc oxide nanoparticles using aqueous extract of *Deverra tortuosa* and their cytotoxic activities. *Sci. Rep.* 10, 3445–3453. <https://doi.org/10.1038/s41598-020-60541-1>.
- Seshadri, R., Rao, C.N.R., A. Muller, A.K. Cheetham (Eds.), *The chemistry of nanomaterials*, Vol. 1, Wiley-VCH Verlag GmbH, Weinheim 2004, pp. 94–112.
- Stan, M., Popa, A., Toloman, D., Silipas, T.D., Vodnar, D.C., 2016. Antibacterial and antioxidant activities of ZnO nanoparticles synthesized using extracts of *Allium sativum*, *Rosmarinus officinalis* and *Ocimum basilicum*. *Acta Met. Sin. Engl. Lett.* 29, 228–236. <https://doi.org/10.1007/s40195-016-0380-7>.
- Stuart, B., 2004. *Infrared Spectroscopy: Fundamentals and Applications*. John Wiley & Sons, Inc., England.
- Supraja, N., Prasad, T.N.K., Krishna, T.G., David, E., 2016. Synthesis, characterization, and evaluation of the antimicrobial efficacy of *Boswellia ovalifoliolata* stem bark-extract-mediated zinc oxide nanoparticles. *Appl. Nanosci.* 6, 581–590. <https://doi.org/10.1007/s13204-015-0472-0>.
- Swee-Yong, P., Lee, W.-P., Aziz, A., 2012. Kinetic study of organic dye degradation using ZnO particles with different morphologies as a photocatalyst. *Int. J. Inorg. Chem.* 2012, 1–9. <https://doi.org/10.1155/2012/608183>.
- Wang, R.H., Xin, J.H., Tao, X.M., Daoud, W.A., 2004. ZnO nanorods grown on cotton fabrics at low temperature. *Chem. Phys. Lett.* 398, 250–255. <https://doi.org/10.1016/j.cplett.2004.09.077>.
- Yusof, H.M., Mohamad, R., Zaidan, U.H., Abdul Rahman, N.A., 2020. Sustainable microbial cell nanofactory for zinc oxide nanoparticles production by zinc-tolerant probiotic *Lactobacillus plantarum* strain TA4. *Microb. Cell Fact.* 19, 1–17. <https://doi.org/10.1186/s12934-020-1279-6>.
- Yusof, H.M., Mohamad, R., Zaidan, U.H., 2019. Microbial synthesis of zinc oxide nanoparticles and their potential application as an antimicrobial agent and a feed supplement in animal industry: a review. *J. Anim. Sci. Biotechnol.* 10, 57. <https://doi.org/10.1186/s40104-019-0368-z>.